

JCTC

Journal of Chemical Theory and Computation

A Consistent Force Field for the Carboxylate Group

Maxim Tafipolsky and Rochus Schmid*

*Lehrstuhl für Anorganische Chemie 2, Organometallics and Materials Chemistry,
Ruhr-Universität Bochum, Universitätsstr. 150, D-44780 Bochum, Germany*

Received June 16, 2009

Abstract: In the light of the important role played by the carboxylate group in bio- and coordination chemistry, its consistent and reliable parametrization for molecular simulations is crucial. The experimental vibrational spectra of three carboxylate anions (formate, acetate, and benzoate) both in the gas phase and in the condensed phase (as sodium salts) are interpreted on the basis of high-quality ab initio calculations. The interaction with the counterion (metal cation) is shown to be of major importance in the interpretation of the spectral features of the carboxylate group both in the solid state and in aqueous solution. Previous attempts to parametrize the carboxylate group within the molecular mechanics approach is critically reviewed, and a new set of the consistent valence force field parameters based on first principles calculations is proposed, which is able to reproduce accurately both the structure and the dynamics of the carboxylate moiety both free and coordinated with metal cations.

1. Introduction

Despite the fact that the carboxylate group is an important functionality abundant in biological systems, being one of the major intracellular anions, its parametrization within the molecular mechanics (MM) approach has been rarely done consistently. If both the structure and dynamics of the carboxylate group, either free (isolated) or chelated with metal ions, are required, then a systematic derivation of the force field (FF) parameters is needed. In the course of the development of a FF for the relatively new class of nanoporous metal–organic frameworks (MOFs),¹ we have faced the problem of accurate parametrization of the metal–carboxylate interactions, which are crucial for understanding the structural, thermal, and elastic properties of these materials. Unfortunately, the parameters available in the literature are not able to deliver reliable dynamic quantities (e.g., vibrational frequencies). Hence, there is a need for a systematic strategy for the parametrization of this important organic group.

Interestingly, the most simple carboxylate anion, formate, was used in the late 1980s as an example to demonstrate the usefulness of using first principles calculations for the derivation of FF parameters either alone² or in combination with experimental data.³ Since then, a number of attempts

have been aimed at the development of the parameters for the carboxylate group using various functional forms. Utilizing a “building block” approach, where any large system is broken down structurally into key functional components, which were parametrized separately, Kirschner et al.⁴ have studied the conformational flexibility of amino acid zwitterions on the basis of their parameters for the carboxylate group derived within the MM3 force field. To develop force constants, they used Møller–Plesset second-order (MP2) perturbation calculations on small carboxylates. Whereas structural data were well reproduced, their inability to match vibrational frequencies of the carboxylate group (mainly symmetric and asymmetric stretchings), as will be shown below, was due to the absence of some important interactions (cross-terms) between internal coordinates in the MM3 energy expression, such as the stretch–stretch term. We should note, however, that the importance of these cross-terms has been recognized, and they were implemented in the MM4 force field⁵ for the conjugated systems like benzene and butadiene. Moreover, Lii⁶ in his study based on the MM4 force field has shown that including the C–O/C–O stretch–stretch cross-term improves significantly the agreement with the high-level ab initio calculated frequencies (B3LYP/6-31G(d, p)) for carboxylic acids. Below, we will show that this particular cross-term plays a crucial role in

* Corresponding author e-mail: rochus.schmid@rub.de.

correctly reproducing the C–O stretchings in the carboxylate group as well.

Making use of first principles calculations as the basis for the FF development, one has to be sure that a chosen level of theory is reliable; that is, the results produced are in agreement with high-quality experimental data within specified uncertainties. Recently, thanks to experimental advances, accurate experimental vibrational frequencies for the free carboxylate anions became available. Forney et al.⁷ investigated by IR spectroscopy some important fundamental vibrations of the formate anion and its deuterated analog trapped in a solid neon matrix at 5 K, whereas Oomens and Steill, using infrared multiple photon dissociation action spectroscopy, observed, for the first time, the stretching modes of the free benzoate⁸ and acetate⁹ anions in the gas phase.

The carboxylate moiety is known to have a very diagnostic infrared fingerprint: the symmetric and asymmetric C–O stretch modes are extremely sensitive to the environment.¹⁰ These modes, and in particular their separation, have therefore been widely used in condensed-phase spectroscopic studies to determine the coordination mode in carboxylate salts and solutions.^{10–12} Since some parametrizations were based on the experimental data (structure and frequencies) measured for the condensed phase, the bias due to the environment should be accounted for (counterions or solvent).

In this work, to derive the needed FF parameters, we use the results of first principles calculations, the reliability of which is judged from a comparison with experimental data and other high-level calculations where available.

2. Force Field Derivation

Our model systems include three anions, formate, acetate, and benzoate, and their chelated complexes with alkali (Li and Na) and transition metal (Cu and Zn) cations. Their geometries were fully optimized by a number of methods ranging from density functional theory (DFT), Møller–Plesset second-order (MP2) perturbation theory,¹³ and coupled-cluster (CCSD¹⁴ and CCSD(T)¹⁵) theory. As DFT, we use the hybrid functional, B3LYP.^{16–18} Only valence electrons were correlated in the coupled-cluster calculations. The augmented correlation consistent basis sets, aug-cc-pVXZ (X = D, T, Q),¹⁹ were employed for all atoms if not stated otherwise. For the Zn and Cu atoms, energy-consistent pseudopotentials denoted as (aug-)cc-pVXZ-PP (X = D, T),^{20–22} obtained from the William R. Wiley Environmental Molecular Sciences Laboratory Basis Set Exchange,^{23,24} were employed. In addition to the calculations in a vacuum, the conductor polarizable continuum model (CPCM) was used to take the effects of a dielectric medium (water) into account, with the cavity represented by the United Atom Topological Model applied on radii optimized for the PBE0/6-31G(d) level of theory (RADII = UAKS). All calculations were carried out with the Gaussian program package.²⁵ The optimized structures were confirmed to be true minima by vibrational frequency calculations. Anharmonic frequencies were calculated by numerical differentiation along normal modes as implemented in the Gaussian program package.²⁶

At the optimized geometries, the Hessian matrices in Cartesian coordinates were calculated using analytical second derivatives and then projected into a redundant set of internal coordinates by means of the Moore–Penrose generalized inverse technique and further used in the derivation of the FF parameters. By transforming the Hessian matrix from Cartesian to internal coordinates, rows of the **B** matrix that correspond to translations and rotations (Eckart coordinates) are formed, and the Hessian matrix is orthogonalized with respect to these coordinates such that both translational and rotational degrees of freedom are completely projected out.

The functional form of the MM3(2000) force field of Allinger et al.²⁷ was used as implemented in the TINKER program package.²⁸ We have modified the original MM3 stretch–bend cross-term by introducing two different force constants, k_{sb}^a and k_{sb}^b , for two bonds that comprise the same bond angle as suggested by Mapple et al.²⁹ and implemented a new stretch–stretch cross-term in the form used previously.^{5,6,29} Their functional forms are given below, where r_{ref} and α_{ref} are the reference values for the bond length and bond angle, respectively:

For stretch–stretch cross-terms:

$$E_{ss} = k_{ss}(r^a - r_{ref}^a)(r^b - r_{ref}^b) \quad (1)$$

and for stretch–bend cross-terms:

$$E_{sb} = k_{sb}^a(r^a - r_{ref}^a)(\alpha - \alpha_{ref}) + k_{sb}^b(r^b - r_{ref}^b)(\alpha - \alpha_{ref}) \quad (2)$$

We concentrate on the FF parameters pertaining to the carboxylate group, namely, C–O stretchings, O–C–O in-plane and out-of-plane bendings, and (for the benzoate anion) twisting around the C_{carb}–C_{ph} bond. Our strategy is to project both structural and curvature (Hessian matrix) data into the redundant internal coordinate system. From a practical point of view, the use of redundant coordinates is advantageous, since the point group symmetry of the carboxylate moiety and corresponding force field is preserved; that is, all symmetrically equivalent bonds or angles in the group have the same force constants. We avoid any symmetrization (producing a nonredundant set of internal coordinates) or “localization”³⁰ steps (resulting in maximally diagonal force constants in dependent angle-bending coordinates), which is completely in line with the general MM philosophy where redundant coordinates are used. The problem with the angular redundancies does not occur³¹ because all geometry optimizations and Hessian calculations are carried out in Cartesian coordinates, and we use exactly the same (complete) set of internal coordinates in the transformation of the Hessian. In addition, due to the redundancy relationship among the three valence angles around the trigonal-planar C_{carb} atom, the values for some cross-terms (see Figure 1) are reproduced automatically and there is no need to parametrize them explicitly. These are all bend–bend and CO/RCO (and CR/OCO) stretch–bend interactions (R = H, C).

3. Results and Discussion

First, we present and discuss the structural data for the simplest carboxylate, the formate anion, which was the

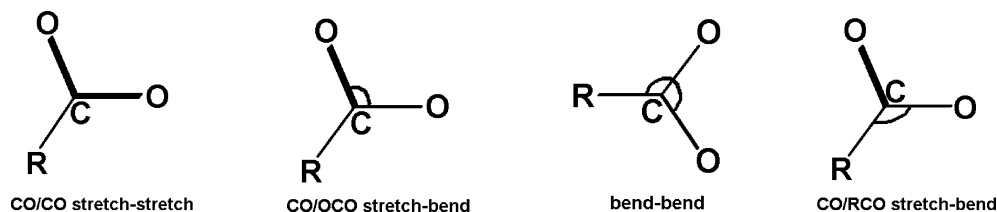


Figure 1. Some important cross-terms in the carboxylate group.

Table 1. Selected Structural Data for the Formate Anion

method	$r(\text{C}-\text{O})$, Å	$\angle\text{O}-\text{C}-\text{O}$, deg
B3LYP/cc-pVDZ	1.2519	131.28
B3LYP/aug-cc-pVDZ	1.2578	130.26
B3LYP/aug-cc-pVTZ	1.2512	130.39
B3LYP/aug-cc-pVQZ	1.2495	130.39
MP2/aug-cc-pVDZ	1.2694	130.15
MP2(full)/aug-cc-pVDZ	1.2685	130.15
MP2/aug-cc-pVTZ	1.2583	130.20
MP2/aug-cc-pVQZ	1.2551	130.15
CCSD/aug-cc-pVDZ	1.2626	130.25
CCSD(T)/aug-cc-pVDZ	1.2689	130.28
MP4/6-311++G(d, p) ^a	1.264	130.48
CCSD(T)/aug-cc-pVTZ ^b	1.258	130.2
CCSD(T)/aug-cc-pVQZ ^c	1.2535	130.18

^a Reference 32. ^b Reference 33. ^c Reference 34.

subject of numerous theoretical investigations. The most recent contributions are by Magalhaes et al.,³² Dixon et al.³³ and Krekeler et al.³⁴ The most important structural parameters calculated at different levels of theory are compared in Table 1.

Using the results from the highest level of theory (CCSD(T)/aug-cc-pV6Z+aug-cc-pV5Z, all electrons correlated) used in the work of Krekeler et al.³⁴ as the benchmark, we note that their values ($r(\text{C}-\text{O}) = 1.2501$ Å and $\angle\text{O}-\text{C}-\text{O} = 130.14^\circ$) can be well reproduced using a much cheaper B3LYP/aug-cc-pVTZ level of theory. Augmentation of the basis set with the diffuse functions has been known for quite a long time to be important for reliable predictions of the properties of anions.³⁵ If we compare the results from our two DFT calculations (see Table 1) with (B3LYP/aug-cc-pVDZ) and without (B3LYP/cc-pVDZ) diffuse functions, the only visible deviation is found for the O-C-O angle ($\sim 1^\circ$). More drastic changes, however, will be seen below when comparing vibrational frequencies (see also ref 32). The influence of the substituent on the structural parameters of the carboxylate group can be seen from the data presented in Table 2.

One clear trend is evident from the calculated results, namely, the C-O bond distance becomes shorter by ~ 0.007 Å on going to a larger basis set. At the same time, one can see no pronounced influence of the substituent on the C-O bond distance. We also note that the stretching of the C-O distances results in the closing of the O-C-O angle.

The calculated vibrational frequencies for the three carboxylate anions are compared with the available experimental data in Table 3. We focus here on three normal modes: the symmetric and asymmetric CO stretching and the OCO bending.

By comparing our calculated vibrational frequencies for the formate anion with those of Krekeler et al.,³⁴ we see

Table 2. Selected Structural Data for the Three Carboxylate Anions

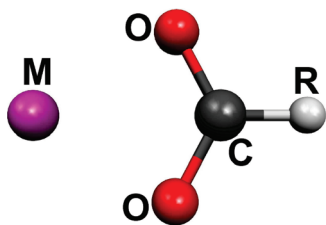
method	$r(\text{C}-\text{O})$, Å	$\angle\text{O}-\text{C}-\text{O}$, deg
Formate		
B3LYP/aug-cc-pVDZ	1.2578	130.26
B3LYP/aug-cc-pVTZ	1.2512	130.39
MP2/aug-cc-pVDZ	1.2694	130.15
MP2/aug-cc-pVTZ	1.2583	130.20
CCSD(T)/aug-cc-pVDZ	1.2689	130.28
Acetate		
B3LYP/aug-cc-pVDZ	1.2618	128.55
B3LYP/aug-cc-pVTZ	1.2548	128.75
MP2/aug-cc-pVDZ	1.2720	128.64
MP2/aug-cc-pVTZ	1.2609	128.76
CCSD(T)/aug-cc-pVDZ	1.2715	128.73
Benzoate		
B3LYP/aug-cc-pVDZ	1.2591	129.14
B3LYP/aug-cc-pVTZ	1.2524	129.23
MP2/aug-cc-pVDZ	1.2688	129.48

that the B3LYP/aug-cc-pVTZ level of theory is quite adequate for describing dynamics within the carboxylate moiety. Importantly, the harmonic frequencies should be corrected for anharmonicity effects in order to be in agreement with experimental results. This correction is, however, different for various modes. In our case, both symmetric and asymmetric CO stretching modes are appreciably affected by anharmonicity (~ 30 cm⁻¹), whereas the OCO bending is almost not affected. Overall, very good agreement between our corrected values and the experimental data for the free formate anion gives us confidence in the chosen level of theory (B3LYP/aug-cc-pVTZ). We can reproduce both the absolute values for the CO stretching frequencies and their difference as well (see last column in Table 3). We should note that, whereas the absolute values for the CO stretching frequencies are dependent on the level of theory used, their difference ($\Delta\nu_{\text{as-s}}$, see last column in Table 3) is much less prone to systematic errors, such as basis set truncation, anharmonic correction, and so forth. The calculated frequency separation between the CO asymmetric and symmetric stretchings is, therefore, a reliable diagnostic of the chemical environment of a carboxylate group. This separation has been widely used in spectroscopy to elucidate the type of metal ion coordination to the COO moiety.¹⁰ Assuming similar values for the anharmonic correction for carboxylate stretchings, we can see that the agreement between our calculated values and the experimental ones for the acetate and benzoate anions is fairly good. Even a smaller basis set (B3LYP/aug-cc-pVDZ) can deliver reliable results, as shown recently by Oomens and Steill.⁸ In their work, they stressed the critical role played by diffuse functions in reproducing stretching modes. In the followup study,⁹ all

Table 3. Selected Vibrational Frequencies (in cm^{-1}) for the Three Carboxylate Anions

method	$\delta(\text{OCO})$	$\nu_{\text{as}}(\text{C}-\text{O})$	$\nu_{\text{s}}(\text{C}-\text{O})$	$\Delta\nu_{\text{as-s}}$
Formate				
B3LYP/aug-cc-pVTZ	744 (739) ^a	1649 (1621)	1338 (1312)	311 (309)
CCSD(T)/aug-cc-pVQZ ³⁴	745 (738)	1653 (1619)	1342 (1316)	311 (303)
MP4/6-311++G(d, p) ³²	726	1626	1294	332
exptl ⁷	744	1629	1323	306
Acetate				
B3LYP/aug-cc-pVTZ	863 (838) ^b	1638 (1605)	1347 (1306) ^b	291 (299)
exptl ⁹	835	1590	1305	285
Benzoate				
B3LYP/aug-cc-pVTZ	813 ^b	1662	1335 ^b	327
exptl ⁸	804	1626	1311	315

^a Anharmonic frequencies are given in parentheses. ^b With the significant contribution from the $\text{C}_{\text{carb}}-\text{C}$ stretching.

**Figure 2.** Bidentate complex of metal carboxylate.

calculated harmonic frequencies were scaled by a factor of 0.98, thus correcting for anharmonicity effects. Blue-shifting of the OCO bending mode for both acetate and benzoate anions as compared to the formate anion, as seen from the data presented in Table 3, is mainly due to the strong coupling with the $\text{C}_{\text{carb}}-\text{C}(\text{R})$ stretching mode.

Having established a reliable computational framework, it is of importance to go beyond the free anions and to try to simulate the carboxylate moiety in its complexes with metals or in condensed phases where the anion is surrounded by counterions or solvent molecules. Interestingly, various previous attempts to interpret the IR and Raman spectra, measured both in the solid state and in solutions, in terms of the carboxylate fingerprints failed for one or another reason. We argue that taking the counterion (alkali metal cation) into account can explain the main features of the spectra pointing to the minor role played by the solvent. To this end, we have fully optimized the geometry of the carboxylate anions chelated in a simple bidentate fashion by the sodium cation (see Figure 2). The structural data and vibrational frequencies are given in Table 4.

Such a “direct binding”³⁶ is frequently found in the crystal structures of anhydrous alkali metal salts of formate and acetate (see, for example refs 37–39) or of more complex carboxylates.⁴⁰ Recently, Aziz et al.⁴¹ have probed directly the contact ion pair interaction using oxygen K-edge X-ray absorption spectroscopy and molecular dynamics simulations and were able to show that this symmetric bidentate coordination prevails in the aqueous solution of sodium acetate. We note, however, that local environments around a metal cation and a carboxylate group in the crystal structure of sodium acetate trihydrate^{42,43} are different from those found in its three anhydrous polymorphs.^{37,44} Similar spectral features observed in the solid state of sodium acetate trihydrate and in its aqueous solution can be seen as an

indirect indication of a similar local environment around an acetate moiety in the condensed phase.

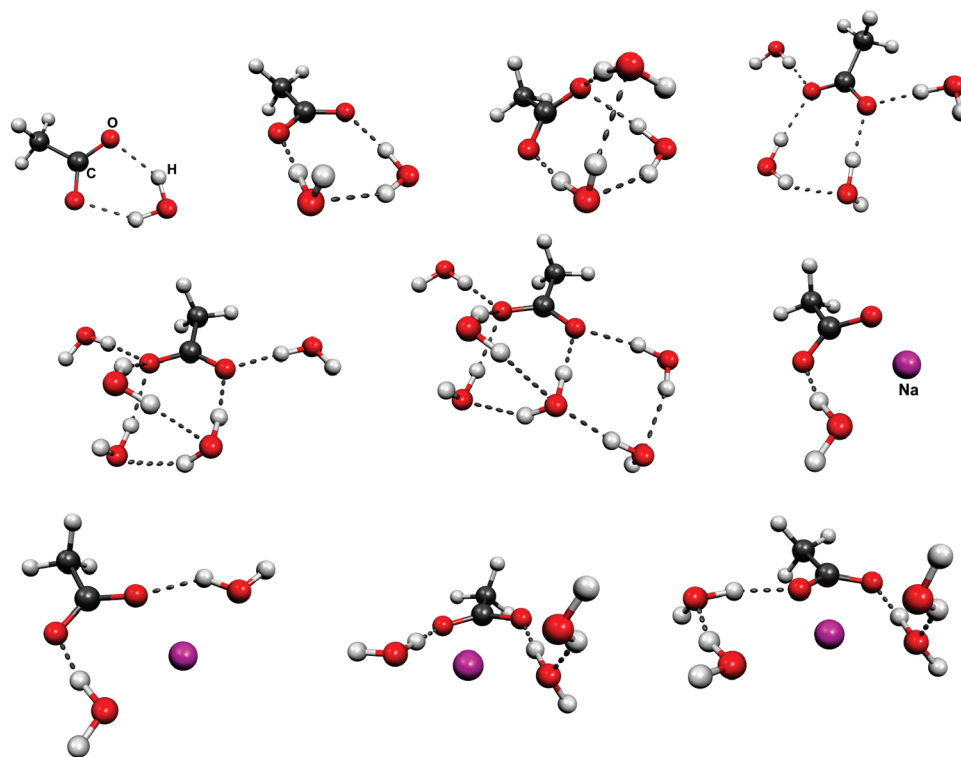
Comparing the structural parameters of the free carboxylates (see Table 1) with those in their sodium complexes, we note that the geometry around the C_{carb} atom is perturbed quite significantly by the presence of the counterion. The calculated $\text{C}-\text{O}$ bond distances are longer than those found in the solid state most probably due to the fact that the $\text{Na}\cdots\text{O}$ distances in the crystal structures are appreciably larger ($2.4\text{--}2.7\text{ \AA}$)^{37,38} than the calculated ones (2.2 \AA), which in turn is a direct consequence of the six-coordinated metal site found in the solid state. In the coordination sphere of the Na cation, two of the six oxygens belong to the same carboxylate (formate or acetate) ion, while the other four oxygens belong to four different ions. Interestingly, the closure of the OCO angle on complexation is well-reproduced by our calculations. From the data presented in Table 4, we confirm the conclusion reached by Keresztury et al.⁵³ on the importance of taking the counterion into account in order to be able to interpret the vibrational spectra of sodium acetate (see also ref 54). We should also note that the asymmetric stretching mode shows up in the solid state spectra with some scatter (see Table 4). This could be due to the fact that anhydrous sodium acetate is known to exist in three different modifications,^{37,44} where a particular atomic arrangement around the acetate anion affects this mode to a larger extent. Taking the solvent (water) implicitly into account within the conductor polarizable continuum model makes the agreement with the experimental frequencies slightly worse. Upon solvation, the most noticeable geometrical change was the lengthening of the $\text{Na}\cdots\text{O}$ distances ($\sim 0.2\text{ \AA}$), which is, of course, due to the large dielectric constant of water (see also ref 55). These enlarged $\text{Na}\cdots\text{O}$ separations are still in the range for a “direct binding” ($2.3\text{--}2.6\text{ \AA}$).^{36,40} It is remarkable that this very simple model for the sodium acetate (also used before) can account for the most salient spectral bands. Since sodium acetate has been the subject of numerous spectroscopic investigations, it is informative to compare more closely the calculated harmonic frequencies with their experimental counterparts available in the literature.^{49,50}

In solution, in contrast to the crystal structures of anhydrous carboxylate salts, the influence of solvent molecules should be taken into account as well. In aqueous solution, for example, hydration by water molecules com-

Table 4. Selected Structural Data and Vibrational Frequencies (in cm^{-1}) for Sodium Carboxylates

method	$r(\text{C}-\text{O})$, Å	$\angle\text{O}-\text{C}-\text{O}$, deg	$\delta(\text{OCO})$	$\nu_{\text{as}}(\text{C}-\text{O})$	$\nu_{\text{s}}(\text{C}-\text{O})$	$\Delta\nu_{\text{as-s}}$
Na-formate						
B3LYP/aug-cc-pVTZ	1.260	125.6	795 (788) ^a	1593 (1560)	1366 (1344)	227 (216)
B3LYP/aug-cc-pVTZ (CPCM)	1.260	125.0	763	1547	1338	209
exptl (solid state) ⁴⁵	1.2560(3) ^b	125.50(3) ^b	773	1595	1359	236
exptl (aq. solution) ⁴⁶			769 ^c	1580	1351	229
Na-acetate						
B3LYP/aug-cc-pVTZ	1.267	123.6	679	1569	1426	143
B3LYP/aug-cc-pVTZ (CPCM)	1.265	123.4	659	1538	1416	122
exptl (solid state) ⁴⁷	1.245, 1.255 ^d	123.6 ^d	650	1580	1424	160
exptl (solid state) ⁴⁸	1.253, 1.257 ^e	123.7 ^e	658	1562	1424	138
exptl (solid state) ⁴⁹	1.250, 1.253 ^f	124.3 ^f	650	1568	1426	142
exptl (aq. solution) ⁴⁶				1550	1416	134
exptl (aq. solution) ⁴⁹			653	1556	1420	136
exptl (aq. solution) ⁵⁰			654	1551	1416	135
Na-benzoate						
B3LYP/aug-cc-pVTZ ^g	1.268	123.4	860	1556	1409	147
exptl (solid state) ⁵¹			845	1552	1413	139
exptl (aq. solution) ⁵¹			845	1545	1391	154

^a Anharmonic frequencies are given in parentheses. ^b Reference 39. ^c Reference 52. ^d Anhydrous sodium acetate.³⁷ ^e Sodium acetate trihydrate.⁴² ^f Sodium acetate trihydrate.⁴³ ^g Basis set without diffuse functions (cc-pVTZ) were used for all H atoms.

**Figure 3.** Optimized clusters of acetate anions with the sodium cation and water molecules (B3LYP/aug-cc-pVDZ). Hydrogen bonds are indicated by dash lines.

petes with cation–anion ion pairing. Therefore, it is quite informative to compare the influence of explicit water molecules with that of a counterion in regard to the structural parameters and vibrational frequencies of the carboxylate moiety. To this end, ab initio calculations (B3LYP/aug-cc-pVDZ) on isolated complexes of the acetate anion with one, two, three, four, five, or six water molecules have been carried out. The exploration of the potential energy hypersurface of these clusters was not exhaustive and served mainly to reveal some trends (if any), and only some stable local minima were identified, shown in Figure 3. Recent ab initio calculations and molecular dynamics simulations

indicate that the average number of water molecules in the proximity of the carboxylate groups in formate and acetate (first coordination shell) is in the range of four to six (see, for example, refs 56–58 and references cited therein). Recent time-of-flight neutron diffraction measurements carried out on aqueous sodium acetate solutions indicated that the first hydration shell of an acetate ion comprises four water molecules.⁵⁹ Interestingly, our results suggest that an acetate anion can accommodate as many as five water molecules but with a tendency to form hydrogen bonds between water molecules if their number increases further (compare clusters with five and six water molecules in Figure 3). This is

Table 5. Selected Vibrational Frequencies (in cm^{-1}) for Sodium Acetate

mode ^a	calcd ^b	exptl (Raman, solid state) ⁴⁹	exptl (Raman, aq. solution) ⁴⁹	exptl (IR, solid state) ^{47,c}
$\nu_{\text{as}}(\text{C}-\text{O})$	1569 (1634)	1568	1556	1580
$\nu_{\text{s}}(\text{C}-\text{O})^d$	1426 (1347)	1426	1420	1424
$\nu(\text{C}-\text{C})$	929 (863)	935	930	923
$\delta(\text{OCO})^d$	679 (630)	650	653	650
$\pi(\text{OCO})$	622 (599)	617	621	625
$\rho(\text{OCO})$	465 (436)	478	480	468

^a The notations ν , δ , ρ , and π are used for the stretching, in-plane bending, rocking, and out-of-plane bending modes, respectively. ^b Harmonic frequencies calculated at the B3LYP/aug-cc-pVTZ level. Values for the free acetate anion are given in parentheses. ^c Anhydrous sodium acetate at 80 K. ^d With a significant contribution from the C–C stretching.

qualitatively in agreement with a recent first-principles (DFT/BLYP) molecular dynamics study of formate anion hydration by Leung and Rempe,⁵⁸ where a hydration number of 2.45 per formate oxygen was predicted. Our findings are also in accord with a recent study of da Silva et al.,⁶⁰ where explicit solvent molecules were used in the continuum model calculations with the conclusion that five water molecules are enough to represent strong solute–solvent interactions exemplified, among others, by the hydration of ionic solutes such as formate and acetate anions. Table 6 lists the most relevant structural parameters and frequencies for the optimized acetate–water clusters.

Some conclusions can be readily drawn from the data on acetate–water clusters. In terms of both structural parameters and vibrational frequencies, adding water molecules produces a noticeable departure from the values for the isolated anion, which is a direct consequence of the hydrogen bonds being formed between acetate and water molecules. The most evident structural changes are the shortening of the C–C bond distance (and the corresponding blue-shift of the C–C stretching frequency) and the decrease of the O–C–O bond angle, which are in agreement with previous ab initio calculations of Markham et al.⁵⁶ The nonequivalence of the two CO bond distances in the clusters with more than one water molecule, due to asymmetric hydrogen bonds, has been pointed out in a recent study by Gojlo et al.⁶¹ (see also refs 12 and 53). The complexation of acetate with one water molecule, the dimer being both experimentally and theoretically well studied (see, for example, refs 62 and 63), does not explain the vibrational features in the carboxylate region observed in an aqueous solution of sodium acetate. We note, however, that, with more water molecules added, an appreciable increase/decrease of the symmetric/asymmetric C–O stretching frequencies becomes evident as compared with the values for the isolated anion. Furthermore, adding one sodium atom to the acetate–water clusters results in the redistribution of the electron charge density within the acetate ion, which manifests itself in a further lowering of the asymmetric C–O stretching frequency and decreasing the frequency separation between the asymmetric and symmetric C–O stretching modes (compare with Table 5). To separate the influence of the cation from that of water molecules to some extent, appropriate crown ethers or cryptands can be used to trap a counterion, thus preventing ion pairing.⁶⁴ A direct structural and spectroscopic study of the microsolvation

of the carboxylate anion can be of great help here (see, for example, ref 65). The optimized sodium–acetate–water complexes with one, two, and four water molecules exhibit an asymmetrical arrangement of the sodium atom with respect to the two carboxylate oxygens with the $\text{Na}\cdots\text{O}(\text{carb})$ distances in the ranges of 2.1–2.3 Å (short contacts) and 3.0–3.6 Å (long contacts). The close contacts between sodium and water molecules in the clusters studied (2.2–2.4 Å) lead to an enhancement of the hydrogen bonding with the carboxylate oxygen atoms thus indirectly influencing the geometry and dynamics of the acetate. This is particularly so in the complex with sodium and three water molecules (see Figure 3), approximately mimicking the local environment around an acetate in the crystal structure of sodium acetate trihydrate,^{42,43} where the two calculated $\text{Na}\cdots\text{O}(\text{carb})$ distances are 3.6 Å and the shortest $\text{H}-\text{O}-\text{H}\cdots\text{O}(\text{carb})$ contact is 1.45 Å, whereas in pure acetate–water clusters, our calculations (B3LYP/aug-cc-pVDZ) give $\text{H}-\text{O}-\text{H}\cdots\text{O}(\text{carb})$ hydrogen bond distances in the range of 1.6–1.8 Å. This means, that reliable interpretation of the spectra of acetate even in aqueous solution is possible only if the counterion is taken into account. Recently, Park and Woon⁶⁶ have studied by DFT (B3LYP/6-31+G(d, p)) the formate anions embedded in water clusters of varying sizes and found that the influence of a counterion (ammonium) should be taken into account to better match the frequencies and intensities of CO stretching modes of the experimental spectra.

Molecular dynamics simulations based on ab initio potentials, which include both the counterions and water molecules explicitly, would be of great help to reliably interpret the structure and dynamics of metal carboxylates in aqueous solution. At present, however, long time simulations utilizing nonempirical potentials are very time-consuming, and therefore, reliable force field parametrizations are of great relevance.

On the basis of the very good overall agreement between our calculated and experimental frequencies, one can conclude that the cation–anion interaction plays an important role both in aqueous solution and in the solid state. We stress, however, that the “free” carboxylate model is incapable of explaining the spectral features observed for metal carboxylates studied here. We note that the inclusion of the effects of solvent implicitly (via CPCM self-consistent field with water as a dielectric medium) perturbed the geometry of the isolated acetate anion quite appreciably; it is, however, not able to reproduce the experimental spectral features (see Table 6). Despite the fact that both structural and vibrational data can be dependent on the particular solvent reaction field model used and other calculational details (see also ref 53), our results point to the necessity to consider (at least) the first hydration shell around acetate explicitly. This can explain a mismatch between the calculated C–O stretching frequencies and those observed in the condensed phase of sodium carboxylates in a recent study by Oomens and Steill,⁹ whereas their calculated values agreed with the experimental frequencies for the isolated carboxylates in the gas phase. In their work, the calculated frequencies have been scaled to account for anharmonic effects and other systematic deficiencies originated from the chosen level of calculation

Table 6. Selected Structural Parameters and Frequencies (in cm^{-1}) for the Optimized Acetate–Water Clusters (B3LYP/aug-cc-pVDZ)

n^a	$r(\text{C}-\text{O}), \text{\AA}$	$\angle \text{O}-\text{C}-\text{O}, \text{deg}$	$r(\text{C}-\text{C}), \text{\AA}$	$\nu_{\text{as}}(\text{C}-\text{O})$	$\nu_{\text{s}}(\text{C}-\text{O})^b$	$\nu(\text{C}-\text{C})$	$\delta(\text{OCO})^b$
0 ^c	1.262	128.6	1.560	1634	1348	865	624
0 (CPCM) ^d	1.269	124.7	1.531	1503	1392	897	639
1	1.265	127.5	1.547	1615	1373	888	638
2	1.258, 1.270	127.6	1.542	1621	1390	888	640
3	1.259, 1.273	126.6	1.536	1608	1397	921	640
4	1.260, 1.272	125.0	1.530	1612	1418	943	659
5	1.262, 1.274	124.5	1.526	1599	1420	931	660
6	1.259, 1.278	124.5	1.524	1598	1420	925	665
1 (Na) ^e	1.268, 1.273	125.1	1.522	1573	1422	923	679
2 (Na) ^e	1.260, 1.277	124.2	1.521	1581	1430	934	678
3 (Na) ^e	1.262, 1.273	126.3	1.523	1568	1427	923	659
4 (Na) ^e	1.260, 1.278	124.0	1.520	1589	1434	920	664

^a Number of water molecules in the cluster (see Figure 3). ^b With the significant contribution from the C–C stretching and other modes.

^c Isolated acetate anion in a vacuum. ^d Isolated acetate anion in a dielectric medium (water). ^e Complex with the sodium cation and water molecules (see Figure 3).

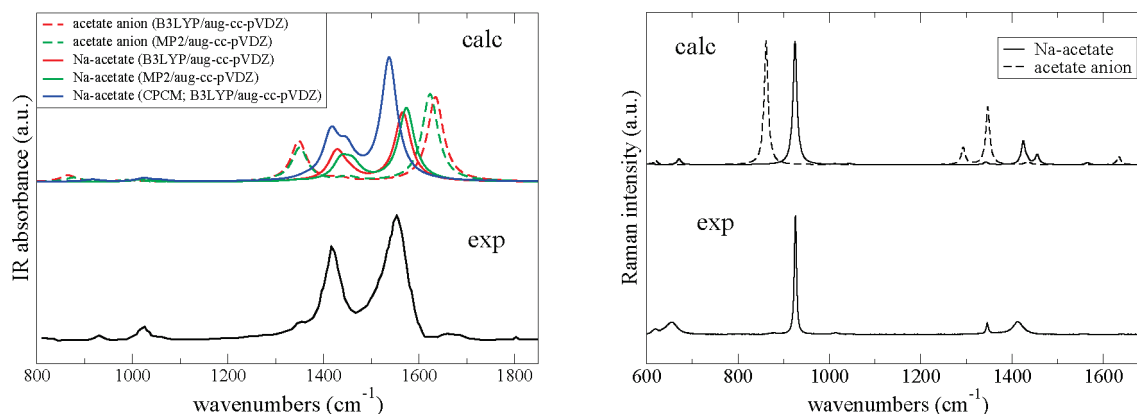


Figure 4. Left: Calculated harmonic IR spectra for the free acetate anion and its sodium bidentate complex. Experimental spectrum for the aqueous solution of sodium acetate is taken from ref 46. Right: Simulated Raman spectra for the acetate anion and its sodium bidentate complex (B3LYP/aug-cc-pVDZ). The wavelength of the diode laser (785 nm), as used in the experiment, is assumed, and line shapes are modeled with the Lorentz function with a resolution of 10 cm^{-1} at room temperature. The experimental Raman spectrum of solid sodium acetate is taken from ref 67.

(see also ref 8). Oomens and Steill,⁹ however, have pointed to the counterion binding as a possible reason for such a discrepancy. As can be seen from our results, upon bidentate metal coordination, the symmetric carboxylate mode is affected much stronger than the asymmetric one. As far as the formate anion is concerned, the large discrepancy between the calculated (free)³² and experimental (aqueous solution) vibrational frequencies can be explained by the influence of the counterion (sodium) present in the condensed phase. The most striking mismatch was observed for the C–H stretching band, where the calculated values of 2657 cm^{-1} (CCSD(T)/aug-cc-pVQZ),³⁴ 2597 cm^{-1} (MP4/6-311++G(d, p)),³² and 2573 cm^{-1} (B3LYP/aug-cc-pVTZ, this work) for the free formate significantly underestimated the values of 2821 cm^{-1} observed in an aqueous solution of its sodium salt⁵² and 2830 cm^{-1} measured for polycrystalline sodium formate.⁴⁵ After correcting the calculated value for anharmonicity (ca. 200 cm^{-1}), Krekeler et al.³⁴ obtained a very good agreement between their frequency (2441 cm^{-1}) and the experimental gas-phase value (2456 cm^{-1}).⁷ Our calculated value (2926 cm^{-1}) for sodium formate (see Figure 2), being corrected for anharmonicity (2748 cm^{-1}), is much closer to the experimental value in aqueous solution mentioned above. This blue-shift of the C–H stretching band is

solely due to the significant shortening of the C–H bond distance upon coordination to a metal cation (1.105 \AA) as compared with the value in the free formate anion (1.135 \AA). This value is in perfect agreement with the low-temperature (120 K) neutron diffraction study on sodium formate of Fuess et al. ($1.1004(7) \text{ \AA}$).³⁹ Contrary to the statement of Dixon et al.,³³ poor agreement is observed between the experimental solid-state frequencies⁴⁵ and their calculated values (CCSD(T)/aug-cc-pVDZ) for the C–H stretching, C–O symmetric stretching, and OCO bending modes since the influence of the counterion (sodium) was ignored.

In Figure 4, we compare the calculated IR and Raman spectra for the free acetate anion and its sodium bidentate complex at different levels of theory. A reduced splitting between the carboxylate asymmetric and symmetric stretching bands is clearly seen for the sodium acetate in the calculated IR spectrum, which reproduces nicely the experimental IR pattern.^{46,50}

It has been shown by Raman spectroscopy^{49,50,68} that the C–C stretching mode in acetate, being the most intense band, is a very sensitive probe of the local chemical environment around the C–C bond. Our calculations (B3LYP/aug-cc-pVDZ) give for this mode a value of 928 cm^{-1} (sodium

Table 7. Projected Force Constants for the Carboxylate Moiety

parameter ^a	free carboxylate			sodium carboxylate		
	formate	acetate	benzoate	formate	acetate	benzoate
C–O str, mdyn/Å	9.83	9.62	9.77	9.51	9.11	9.04
C–R str, mdyn/Å	3.74	3.27	3.48	4.75	4.14	4.44
O–C–O bend, mdyn Å/rad ²	0.80	0.86	0.90	1.01	1.08	1.11
O–C–R bend, mdyn Å/rad ²	0.54	0.72	0.83	0.57	0.74	0.85
O–C–O wag, mdyn Å/rad ²	0.06	0.07	0.07	0.06	0.07	0.07
C–O/C–O str–str, mdyn/Å	1.47	1.52	1.47	1.58	1.59	1.52
C–O/C–R str–str, mdyn/Å	0.63	0.71	0.78	0.40	0.55	0.65
C–O/O–C–O str–bend, mdyn/rad	0.19	0.20	0.21	0.31	0.32	0.34
C–O/O–C–R str–bend, mdyn/rad	0.16	0.20	0.20	0.09	0.13	0.12
C–R/O–C–R str–bend, mdyn/rad	0.12	0.18	0.24	0.08	0.15	0.20
(O, O)C–R tors, mdyn Å/rad ²		0.007	0.06		0.008	0.08

^a Abbreviations used: “str” for stretch; “bend” for in-plane angle bend; “wag” for out-of-plane angle bend; “str–str” and “str–bend” for stretch–stretch and stretch–bend interactions, respectively; and “tors” for COO twisting.

acetate), which deviates appreciably from that found for the free acetate anion (865 cm^{−1}). This is in accord with a much shorter C–C bond distance in the bidentate complex with a sodium cation (1.521 Å) as compared to the value in the isolated acetate (1.560 Å). The simulated Raman spectra for the acetate anion and its sodium bidentate complex, shown in Figure 4, are clearly distinguishable, with the latter being in qualitative agreement with the available experimental data.^{48,67,69}

The interpretation of the Raman bands observed recently from a single supersaturated droplet of sodium acetate by Wang et al.⁷⁰ should probably be reinterpreted. Their band assignment (see Table 1) is in perfect agreement with our results for the sodium bidentate complex if one assumes that, both in dilute solution and in a supersaturated droplet, the acetate group is appreciably perturbed by a counterion.

Having demonstrated the reliability of the chosen computational scheme, we are now in a position to develop the force field parameters, which can be used in molecular simulations where the main focus is on obtaining both accurate geometries and dynamics (vibrational frequencies) of the carboxylate moiety. The derivation of the FF parameters for the formate anion is particularly simple, since, in accord with the MM3 methodology, no van der Waals or electrostatic terms need to be considered (no 1–4 interactions). This is in contrast with the statement of Kirschner et al.,⁴ where difficulties have been encountered when developing parameters for this particular anion. As already mentioned above, this is solely due to the absence of some important cross-terms (stretch–stretch) in the original MM3 functional form.

The calculated Hessian matrix in Cartesian coordinates (B3LYP/aug-cc-pVTZ) was projected into the redundant set of internal coordinates at the trigonal-planar C_{carb} center (three bond stretchings, three in-plane and three out-of-plane angle bendings) both for the free carboxylate ion and for its sodium bidentate complex. The number of parameters to be refined was nine (diagonal terms) and 14 (diagonal and off-diagonal terms).

Besides the influence of the substituent group (R = H, Me, or Ph) clearly seen from the data presented in Table 7, the perturbation of the force constants caused by sodium chelation is also evident. On going from the free carboxylate ion to its complex with the sodium cation, the C–O bond

stretch force constants decrease by ~3% (formate), ~5% (acetate), and ~7% (benzoate), whereas the O–C–O angle in-plane bending force constants increase by ~20%. On the basis of a detailed analysis of the normal modes, the influence of the sodium cation can be described as follows. Since the mode, commonly referred to as “asymmetric” (or sometimes also as “antisymmetric”) stretching, is solely due to the out-of-phase stretching of the two C–O bonds, its frequency should decrease on complexation with the cation simply because the C–O stretch force constant decreases (see Table 7). At the same time, the second mode, commonly referred to as “symmetric” stretching, is actually a mixture of the in-phase stretching of the two C–O bonds and the C–C stretching (in acetate and benzoate) with a small contribution from the O–C–O angle bending. Since both the C–C stretch and the O–C–O angle bend force constants increase on complexation (see Table 7) and, in addition, the contribution from the C–C stretch to this mode increases (from 16% in acetate and benzoate to 26% in sodium acetate and benzoate, on the basis of the potential energy distribution), their overall effect overwhelms the decrease of the C–O stretch force constant, resulting in a higher frequency as compared to that of the free carboxylate anion (compare the data in Tables 3 and 4).

We also found that the rotation around the C_{carb}–C bond in the acetate is essentially free, which is in agreement with previous theoretical^{4,53} and experimental (spectroscopic)⁴⁹ studies. The torsional force constant given by Kakihana et al.⁴⁷ is probably too large, which is due to the overestimation of the barrier to methyl group rotation (2.3 kcal/mol)⁷¹ and that of the corresponding torsional frequency derived therefrom used in the fit. A recent neutron scattering study of Moreno et al.⁷² gave a value of 0.95 kcal/mol for the rotational barrier in anhydrous sodium acetate. This latter value is comparable with that found earlier by Montjoie and Müller-Warmuth⁷³ (0.77 kcal/mol) from their analysis of the correlation between NMR spin–lattice relaxation and neutron-scattering data on anhydrous sodium acetate. The rotational barrier in the benzoate, on the other hand, is appreciable (vide supra).

Introducing two new atomic types, C_{carb} and O_{carb}, and taking minor modifications into account (see eqs 1 and 2), the force field parameters presented in Table 8 are suitable for use within the MM3(2000) force field. As in our previous

Table 8. Additional MM3(2000) Force Field Parameters for the Carboxylate Moiety

Bond Stretches		
atom types	reference distance, Å	force parameter, mdyn/Å
C _{carb} —O _{carb}	1.252 (1.264) ^a	9.8 (9.3)
C _{carb} —H	1.13 (1.11)	3.7 (4.6)
C _{carb} —C(sp ³)	1.542 (1.514)	3.6 (4.2)
C _{carb} —C _{ph}	1.531 (1.481)	3.8 (5.1)
In-Plane Angle Bending		
	reference angle, deg	force parameter, mdynÅ/rad ²
O _{carb} —C _{carb} —O _{carb}	130.0 (124.0)	1.4 (1.9)
O _{carb} —C _{carb} —H	114.8 (114.8)	0.7 (0.7)
O _{carb} —C _{carb} —C(sp ³)	117.3 (117.8)	0.9 (0.9)
O _{carb} —C _{carb} —C _{ph}	115.4 (121.0)	1.0 (0.8)
Out-of-Plane Angle Bending		
(R)—C _{carb} —O _{carb} ^b	0.0	1.7 (1.7)
Stretch—Stretch (mdyn/Å) ^c		
C _{carb} —O _{carb} /C _{carb} —C _{carb}		1.5 (1.6)
C _{carb} —O _{carb} /C _{carb} —R		0.7 (0.5)
Stretch—Bend (mdyn/rad)		
C _{carb} —O _{carb} /O _{carb} —C _{carb} —O _{carb}		0.6 (0.8)
C _{carb} —O _{carb} /O _{carb} —C _{carb} —R		0.6 (0.5)
C _{carb} —R/O _{carb} —C _{carb} —R		0.5 (0.4)

^a Values for a carboxylate moiety perturbed by bidentate coordination of sodium are given in parentheses. ^b All three Wilson angles at a trigonal center are assigned the same force constant. ^c Due to the error in the implementation of eq 1, the values cited in Table 9 of ref 1 should be exactly 2 times smaller.

work,¹ we decided to use effective atomic point charges to describe electrostatic interactions instead of bond dipoles normally used within the MM3 formalism. This is done in order to facilitate the applicability of derived FF parameters within other MM implementations. It turned out, however, that the electrostatic interactions can be ignored since, as we found in our preliminary tests, they had no influence on the parameters we are interested in except for the H—C—C_{carb}—O_{carb} and C_{ph}—C_{ph}—C_{carb}—O_{carb} torsional parameters for acetate and benzoate, respectively. Since the values for the torsional parameters are dependent (especially for benzoate) on the particular electrostatic model used (point charges, bond dipoles, etc.), they are not included in Table 8. The standard MM3(2000) van der Waals parameters were employed without further refinement, since we focus here on intramolecular interactions, and the force field parameters were adjusted with a genetic algorithm used in our previous work.¹

When the atomic point charges fitted to reproduce the electrostatic potential (+0.8 and −0.8 for C_{carb} and O_{carb}, respectively, 0.0 for the C_{ph}(−C_{carb}), and average values of −0.12 and +0.12 for C_{ph}(−H) and H, respectively) were used, and assuming a single 2-fold Fourier term (1/2V₂(1 − cos2φ)) for the C_{ph}—C_{ph}—C_{carb}—O_{carb} twist angle (φ), the parameters V₂ for the isolated benzoate anion and its complex with the sodium cation were refined to be 1.4 and 1.7 kcal/mol, respectively. With these parameters at hand, we reproduce the calculated (B3LYP/aug-cc-pVTZ) lowest (torsional) mode of the isolated benzoate anion (55 cm^{−1}) and its complex with the sodium cation (67 cm^{−1}) within

4 cm^{−1}. If the electrostatic interactions are ignored completely, we arrived at the values of 2.0 and 2.3 kcal/mol, respectively, for the V₂ parameter.

Using the derived FF parameters, the calculated vibrational frequencies for all three carboxylates, characteristic for the carboxylate moiety (symmetric and asymmetric C—O stretchings and O—C—O in-plane bending), are very close to the reference values (B3LYP/aug-cc-pVTZ) with a root-mean-squared deviation of less than 14 cm^{−1}. This is particularly astonishing since, in addition to the diagonal FF parameters, only a few cross-terms (stretch—stretch and stretch—bend) listed in Table 8 were explicitly optimized. Interestingly, due to the redundancy relationship among the three valence angles around the trigonal-planar C_{carb} atom, the values for other cross-terms (see Figure 1) are reproduced automatically. We should note that the importance of the CO/CO stretch—stretch cross-term to reproduce the stretching frequencies of the carboxylate moiety was established by spectroscopists quite a long time ago. Probably, one of the first estimates was due to Jones and McLaren⁷⁴ from the analysis of IR spectra of solid anhydrous sodium acetate (1.7 mdyn/Å), where the structural parameters for the carboxylate group (C—O bond distances and O—C—O bond angle) were taken from the crystal structure of sodium formate.⁷⁵ The values given by Spinner⁷⁶ (1.6 mdyn/Å) and Kidd and Mantsch⁴⁵ (1.6 mdyn/Å) for formate, by Beckmann et al.⁷⁷ (1.3 mdyn/Å) and Kakihana et al.⁴⁷ for acetate (2.0 mdyn/Å), and by Ernstbrunner et al.⁷⁸ for 4-nitrobenzoate (1.5 mdyn/Å) are significant and are very close to the value derived in the present work. We should also mention the large value for this particular stretch—stretch cross-term obtained by Lii⁶ for formic acid (1.3 mdyn/Å). Further, our value for the CO/OCO stretch—bend interaction (in mdyn/rad) is also very similar to those available in the literature (0.3⁴⁵ for formate, 0.4⁷⁷ for acetate, and 0.6⁷⁸ for 4-nitrobenzoate). Relevant to our compilation (see Table 8) are the parameters used to describe the carboxylate group in another widely used MMFF94 force field.⁷⁹ There, the values of 9.756 mdyn/Å, 1.181 mdyn Å/rad², and 0.652 mdyn/rad for the CO bond stretch, OCO angle bend, and CO/OCO stretch—bend interaction, respectively, are used. These values are strikingly similar to those derived in our study. However, no stretch—stretch cross-term is used for this moiety in the MMFF94 force field.

We should mention that, among numerous previous attempts to reproduce the vibrational spectra of carboxylates by refining the corresponding force constants, a particular success of Kakihana et al.⁴⁷ in their study of the acetate anion can be attributed mainly to the use of many important cross-terms in the valence force field (actually, due to the redundancy relationship around the trigonal-planar C_{carb} center, even less cross-terms are needed to parametrize explicitly). Their effective force constants, refined against 82 observed frequencies of six isotopomers of sodium acetate, have implicitly incorporated the influence of the metal cation on vibrational spectra. In another earlier work, Dasgupta and Goddard³ combined the Hessian from ab initio calculations with the structural and spectroscopic data from experimental data to generate the force field parameters for

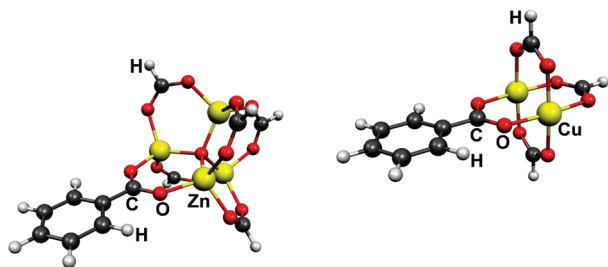


Figure 5. Two motifs encountered in MOFs based on a basic metal carboxylate, $\text{Zn}_4\text{O}(\text{O}_2\text{CH})_5$ -benzoate (left), and a binuclear metal (“paddle-wheel”) carboxylate, $\text{Cu}_2(\text{O}_2\text{CH})_3$ -benzoate (right), building units.

the formate anion. On the basis of their recommended parameters (see Table 2, column labeled as “HTX” in ref 3), we were able to reproduce their large deviation ($\sim 90\text{ cm}^{-1}$) for the lowest-frequency OCO bend (see Table 10, column labeled as “HTX” in ref 3). The reason for this discrepancy could be their smaller values for the OCO bending and CO/OCO stretch–bend interaction force constants as compared to our results.

Our motivation in this work was primarily to develop reliable FF parameters for the carboxylate group directly from the quantum chemical calculations, which can be used in molecular simulations of MOF materials, where this particular functionality is used to link various metal–oxide clusters together, resulting in a 3D porous framework.¹ Among the variety of linkers used so far, one ubiquitous type consists of the carboxylate functionality conjugated with the phenyl moiety,⁸⁰ for which benzoate can serve as a model system. In modeling the frameworks we are interested in, one important parameter is the barrier to internal rotation of the carboxylate group with respect to the phenyl ring. In contrast to the bidentate coordination of an alkali metal (see Figure 2), metal–oxide clusters usually bind in a bridging fashion exemplified in Figure 5 by two representative motifs encountered in MOFs based on basic metal carboxylate and dinuclear metal tetracarboxylate (“paddle-wheel” motif) building units.

In our calculations, the use of the benzoate moiety instead of a more realistic linker encountered in various MOFs, such as benzene-1,4-dicarboxylate (terephthalate) in MOF-5⁸¹ or benzene-1,3,5-tricarboxylate (trimesate) in CuBTC,⁸² needs to be justified. Moreover, replacing the bridging metal–oxide cluster (as shown in Figure 5) with the bidentate coordination of an alkali metal can in principle modify the barrier to rotation as well. To this end, the geometry of an “orthogonal” conformer was optimized, constrained to have the carboxylate group rotated by 90° with respect to the phenyl ring. The torsional barrier was calculated as the energy difference between the global minimum (all atoms are in one plane) and the orthogonal conformer at the B3LYP level of theory using the correlation consistent basis sets of improved quality (from double- to triple- ζ).

The results presented in Table 9 allow some important conclusions to be drawn. First, the augmentation of basis sets with diffuse functions (marked with the prefix “aug”) has a large effect on the barrier, especially for the free benzoate anion. Second, going to a larger basis set lowers

Table 9. Calculated Barriers to Rotation of the Carboxylate Group (kcal/mol) for Model Systems

	cc-pVDZ	aug-cc-pVDZ	cc-pVTZ	aug-cc-pVTZ ^a
benzoate anion	8.2 (8.6) ^b	4.0 (4.5)	5.2 (6.0)	3.8 (4.6)
Li-benzoate	8.1 (7.7)	6.8 (6.3)	7.1 (6.9)	6.8
Na-benzoate	7.9 (7.5)	6.2 (5.9)	6.4 (6.4)	6.0
$\text{Zn}_4\text{O}(\text{O}_2\text{CH})_5$ -benzoate	8.4	6.9	7.0	
$\text{Cu}_2(\text{O}_2\text{CH})_3$ -benzoate ^c	7.5	6.3	6.4	

^a A basis set without diffuse functions (cc-pVTZ) was used for all H atoms. ^b Values calculated at the MP2(frozen core) level of theory are given in parentheses. ^c Triplet electronic state.

Table 10. Calculated Barriers to Rotation of the Carboxylate Group (kcal/mol) for Terephthalate and Trimesate Anions and Their Salts^a

	1	2	3
terephthalate anion	4.2	9.2	
Li_2 -terephthalate	6.4	13.5	
Na_2 -terephthalate	5.8	12.5	
trimesate anion	2.0	4.9	8.4
Li_3 -trimesate	6.1	12.8	19.9
Na_3 -trimesate	5.4	11.4	17.9

^a Numbers (1, 2, or 3) indicate the number of COO groups orthogonal to the benzene plane.

the barrier. Third, a triple- ζ basis set (aug-cc-pVTZ) gives similar results as a much more economical double- ζ basis set (aug-cc-pVDZ). Therefore, the latter basis set can be recommended. We also note that the barriers calculated at the MP2 level of theory using the aug-cc-pVDZ basis set are close to the values obtained at the DFT/B3LYP level. Interestingly, the rotational barriers calculated for bidentate lithium and sodium benzoates are similar to those of bridging zinc and copper benzoates (see Figure 5), respectively. It is also evident that coordination with metals (or metal–oxides) makes the rotational barrier higher in comparison with that in the free carboxylate. To the best of our knowledge, there is no systematic study on the barrier to rotation of the carboxylate group conjugated with aromatic rings and its dependence on the mode of coordination to metal cations. Rakitin and Pack⁸³ have calculated a barrier of 3.4 kcal/mol for the free benzoate anion (MP2/STO-3G), whereas Woo et al.⁸⁴ gave a value of ~ 4.5 kcal/mol for the p-methylbenzoate anion (B3LYP/6-31+G(d, p)).

To get some more insight into the rotational flexibility of the carboxylate group conjugated with the benzene ring, we have calculated (B3LYP/aug-cc-pVDZ) the most important stationary points on potential energy hypersurfaces of terephthalate and trimesate, both as free anions and as chelated (bidentate) complexes with alkali metals (lithium and sodium). The results for rotational isomers (conformers) are presented in Table 10, where the plane of one or two (terephthalate) and one, two, or three (trimesate) COO groups can be orthogonal to the plane of the benzene ring. The energies are given with respect to the global minimum structure, which corresponds to a planar arrangement of all atoms.

The most evident trend seen from these data is that the energy penalty for two (terephthalate) and for two and three (trimesate) orthogonal COO groups is not quite additive; that

is, the energy cost increases with more carboxylate groups rotated out of the benzene plane. Comparing the calculated barriers (B3LYP/aug-cc-pVDZ) in dilithium (13.5 kcal/mol) and disodium (12.5 kcal/mol) terephthalate (in this case, an “orthogonal” conformer corresponds to the geometry where both COO groups are rotated by 90° with respect to the phenylene ring) with the doubled value calculated for lithium ($2 \times 6.8 = 13.6$ kcal/mol) and sodium ($2 \times 6.2 = 12.4$ kcal/mol) benzoates (see Table 9), one can conclude that the energy penalty arising from the rotation of the carboxylate group out of the benzene plane is additive to a large degree. This observation justifies the use of benzoate as a model system for more complicated benzene polycarboxylates such as terephthalate or trimesate. We also note that the calculated torsional barrier is much closer to a recently determined experimental value of 11 ± 2.0 kcal/mol⁸⁵ as compared to our previous estimation (~ 16 kcal/mol; B3LYP/cc-pVDZ),¹ which is due to a larger basis set used in this work (augmented with diffuse basis functions). For some recent estimations of the rotational barriers, see also ref 86.

4. Conclusions

In summary, we have clarified the role played by a counterion in the interpretation of the vibrational spectra of the carboxylate group in the condensed phase (aqueous solution and solid state) using formate, acetate, and benzoate and their sodium bidentate complexes as examples. We have shown that, with the help of such simplified models, it is possible to explain the most salient features observed in spectral regions characteristic of the carboxylate vibrations. In light of new experimental data corroborated by the calculations, the notion of a “free” (isolated) carboxylate needs to be revised. Even in dilute (aqueous) solutions, a carboxylate group can be perturbed by a counterion quite appreciably. We argue that the direct or indirect influence of a counterion was largely underestimated in the past and cannot be ignored. On the basis of the results of ab initio calculations, the changes in the force field of the carboxylate moiety upon metal ion coordination are analyzed in detail. With the use of density functional theory along with a large basis set augmented with diffuse basis functions, the molecular-mechanical force field parameters are developed, aimed at molecular simulations of large biomolecules, such as amino acids, as well as that of a broad class of metal–organic coordination polymers where polydentate carboxylates are used as organic linkers.¹ The use of a complete (redundant) set of internal coordinates is not only a straightforward and natural approach to developing the FF parameters but, in addition, can reduce the number of cross-terms necessary to reliably predict the vibrational frequencies within the MM approach, thus avoiding complications arising from utilizing some additional terms, like the Urey–Bradley term.⁵⁴ In addition to the CO/OCO stretch–bend cross-term, the importance of the CO/CO stretch–stretch interaction in the carboxylate moiety is emphasized. A similar approach can be applied for molecular-mechanical force field derivation for other important anions like phosphate, nitrate, sulfate, carbonate, and so forth. We can anticipate that the presented analysis and derived parameters will be useful in the

modeling of solid metal carboxylates per se,⁸⁷ where not only the structure but, in addition, accurate dynamics are of interest. Simulations of transition metal carboxylates within the MM approach⁸⁸ can also benefit from our findings. With the use of the results of this study, the influence of a particular mode of metal coordination to a carboxylate group, as manifests itself in the fingerprint region of vibrational spectra, can be modeled reliably and accurately, helping to interpret IR spectra of various MOFs. Last but not least, molecular simulations of amino acids in solution (e.g., as zwitterions in water) can be performed by taking full internal flexibility of the carboxylate moiety in the force field into account.

Acknowledgment. The Alfred Krupp von Bohlen und Halbach Stiftung and the Deutsche Forschungsgemeinschaft (SFB-558) are acknowledged for their financial support of this project.

References

- (1) Tafipolsky, M.; Schmid, R. *J. Phys. Chem. B* **2009**, *113*, 1341.
- (2) Maple, J. R.; Dinur, U.; Hagler, A. T. *Proc. Natl. Acad. Sci. U.S.A.* **1988**, *85*, 5350.
- (3) Dasgupta, S.; Goddard, W. A. *J. Chem. Phys.* **1989**, *90*, 7207.
- (4) Kirschner, K. N.; Lewin, A. H.; Bowen, J. P. *J. Comput. Chem.* **2003**, *24*, 111.
- (5) Nevins, N.; Chen, K.-S.; Allinger, N. L. *J. Comput. Chem.* **1996**, *17*, 669.
- (6) Lii, J.-H. *J. Phys. Chem. A* **2002**, *106*, 8667.
- (7) Forney, D.; Jacox, M. E.; Thompson, W. E. *J. Chem. Phys.* **2003**, *119*, 10814.
- (8) Oomens, J.; Steill, J. D. *J. Phys. Chem. A* **2008**, *112*, 3281.
- (9) Steill, J. D.; Oomens, J. *J. Phys. Chem. A* **2009**, *113*, 4941.
- (10) Deacon, G. B.; Phillips, R. J. *Coord. Chem. Rev.* **1980**, *33*, 227.
- (11) Lewandowski, W.; Kalinowska, M.; Lewandowska, H. *J. Inorg. Biochem.* **2005**, *99*, 1407.
- (12) Nara, M.; Torii, H.; Tasumi, M. *J. Phys. Chem.* **1996**, *100*, 19812.
- (13) Möller, C.; Plesset, M. S. *Phys. Rev.* **1934**, *46*, 618.
- (14) Purvis, G. D.; Bartlett, R. J. *J. Chem. Phys.* **1982**, *76*, 1910.
- (15) Pople, J. A.; Head-Gordon, M.; Raghavachari, K. *J. Chem. Phys.* **1987**, *87*, 5968.
- (16) Becke, A. D. *Phys. Rev. A* **1988**, *38*, 3098.
- (17) Becke, A. D. *J. Chem. Phys.* **1993**, *98*, 5648.
- (18) Lee, C.; Yang, W.; Parr, R. G. *Phys. Rev. B* **1988**, *37*, 785.
- (19) Dunning, T. H. *J. Chem. Phys.* **1989**, *90*, 1007.
- (20) Wilson, A. K.; Woon, D. E.; Peterson, K. A.; Dunning, T. H. *J. Chem. Phys.* **1999**, *110*, 7667.
- (21) Figgen, D.; Rauhut, G.; Dolg, M.; Stoll, H. *Chem. Phys.* **2005**, *311*, 227.
- (22) Peterson, K. A.; Puzzarini, C. *Theor. Chem. Acc.* **2005**, *114*, 283.
- (23) Feller, D. *J. Comput. Chem.* **1996**, *17*, 1571.
- (24) Schuchardt, K. L.; Didier, B. T.; Elsethagen, T.; Sun, L.; Gurumoorhi, V.; Chase, J.; Li, J.; Windus, T. L. *J. Chem.*

- Inf. Model.* **2007**, 47, 1045. Accessible at <https://bse.pnl.gov/bse/portal> (accessed August 2009).
- (25) Frisch, M. J.; Trucks, G. W.; Schlegel, H. B.; Scuseria, G. E.; Robb, M. A.; Cheeseman, J. R.; Montgomery, J. A., Jr.; Vreven, T.; Kudin, K. N.; Burant, J. C.; Millam, J. M.; Iyengar, S. S.; Tomasi, J.; Barone, V.; Mennucci, B.; Cossi, M.; Scalmani, G.; Rega, N.; Petersson, G. A.; Nakatsuji, H.; Hada, M.; Ehara, M.; Toyota, K.; Fukuda, R.; Hasegawa, J.; Ishida, M.; Nakajima, T.; Honda, Y.; Kitao, O.; Nakai, H.; Klene, M.; Li, X.; Knox, J. E.; Hratchian, H. P.; Cross, J. B.; Adamo, C.; Jaramillo, J.; Gomperts, R.; Stratmann, R. E.; Yazyev, O.; Austin, A. J.; Cammi, R.; Pomelli, C.; Ochterski, J. W.; Ayala, P. Y.; Morokuma, K.; Voth, G. A.; Salvador, P.; Dannenberg, J. J.; Zakrzewski, V. G.; Dapprich, S.; Daniels, A. D.; Strain, M. C.; Farkas, O.; Malick, D. K.; Rabuck, A. D.; Raghavachari, K.; Foresman, J. B.; Ortiz, J. V.; Cui, Q.; Baboul, A. G.; Clifford, S.; Cioslowski, J.; Stefanov, B. B.; Liu, G.; Liashenko, A.; Piskorz, P.; Komaromi, I.; Martin, R. L.; Fox, D. J.; Keith, T.; Al-Laham, M. A.; Peng, C. Y.; Nanayakkara, A.; Challacombe, M.; Gill, P. M. W.; Johnson, B.; Chen, W.; Wong, M. W.; Gonzalez, C.; Pople, J. A. *Gaussian 03*, revision B.04; Gaussian, Inc.: Pittsburgh, PA, 2003.
- (26) Barone, V. *J. Chem. Phys.* **2005**, 122, 014108.
- (27) Allinger, N. L.; Yuh, Y. H.; Lii, J.-H. *J. Am. Chem. Soc.* **1989**, 111, 8551.
- (28) Ponder, J. W.; Ren, P.; Pappu, R. V.; Hart, R. K.; Hodgson, M. E.; Cistola, D. P.; Kundrot, C. E.; Richards, F. M. *TINKER*, version 4.2; Washington University School of Medicine: St. Louis, MO, 2004 Available at <http://dasher.wustl.edu/tinker/> (accessed August 2009).
- (29) Maple, J. R.; Hwang, M. J.; Stockfisch, T. P.; Dinur, U.; Waldman, M.; Ewig, C. S.; Hagler, A. T. *J. Comput. Chem.* **1994**, 15, 162.
- (30) Halgren, T. A. *THEOCHEM* **1988**, 163, 431.
- (31) Palmo, K.; Pietila, L.-O.; Krimm, S. *J. Comput. Chem.* **1992**, 13, 1142.
- (32) Magalhaes, A. L.; Madail, S. R. R. S.; Ramos, M. J. *Theor. Chem. Acc.* **2000**, 105, 68.
- (33) Dixon, D. A.; Feller, D.; Francisco, J. S. *J. Phys. Chem. A* **2003**, 107, 186.
- (34) Krekeler, C.; Mladenovic, M.; Botschwina, P. *Phys. Chem. Chem. Phys.* **2005**, 7, 882.
- (35) Clark, T.; Chandrasekhar, J.; Spitznagel, G. W.; Schleyer, P. v. R. *J. Comput. Chem.* **1983**, 4, 294.
- (36) Carrell, C. J.; Carrell, H. L.; Erlebach, J.; Glusker, J. P. *J. Am. Chem. Soc.* **1988**, 110, 8651.
- (37) Hsu, L. Y.; Nordman, C. E. *Acta Crystallogr., Sect. C* **1983**, 39, 690.
- (38) Markila, P. L.; Rettig, S. J.; Trotter, J. *Acta Crystallogr., Sect. B* **1975**, 31, 2927.
- (39) Fuess, H.; Bats, J. W.; Dannohl, H.; Meyer, H.; Schweig, A. *Acta Crystallogr., Sect. B* **1982**, 38, 736.
- (40) Glusker, J. P. *Acta Crystallogr., Sect. D* **1995**, 51, 418.
- (41) Aziz, E. F.; Ottosson, N.; Eisebitt, S.; Eberhardt, W.; Jagoda-Cwiklik, B.; Vacha, R.; Jungwirth, P.; Winter, B. *J. Phys. Chem. B* **2008**, 112, 12567.
- (42) Wei, K. T.; Ward, D. L. *Acta Crystallogr., Sect. B* **1977**, 33, 522.
- (43) Efremov, V. A.; Endeladze, N. O.; Agre, V. M.; Trunov, V. K. *J. Struct. Chem.* **1986**, 27, 498.
- (44) Helmholtz, R. B.; Sonneveld, E. J.; Schenk, H. Z. *Kristallogr.* **1998**, 213, 596.
- (45) Kidd, K. G.; Mantsch, H. H. *J. Mol. Spectrosc.* **1981**, 85, 375.
- (46) Pike, P. R.; Sworan, P. A.; Cabaniss, S. E. *Anal. Chim. Acta* **1993**, 280, 253.
- (47) Kakihana, M.; Kotaka, M.; Okamoto, M. *J. Phys. Chem.* **1983**, 87, 2526.
- (48) Frost, R. L.; Klopprogge, J. T. *J. Mol. Struct.* **2000**, 526, 131.
- (49) Bickley, R. I.; Edwards, H. G. M.; Rose, S. J.; Gustar, R. J. *Mol. Struct.* **1990**, 238, 15.
- (50) Quiles, F.; Burneau, A. *Vib. Spectrosc.* **1998**, 16, 105.
- (51) Green, J. H. S. *Spectrochim. Acta, Part A* **1977**, 33, 575.
- (52) Spinner, E. *J. Chem. Soc. B* **1967**, 879.
- (53) Keresztury, G.; Istvan, K.; Sundius, T. *J. Phys. Chem. A* **2005**, 109, 7938.
- (54) Mezziane-Tani, M.; Lagant, P.; Semmoud, A.; Vergoten, G. *J. Phys. Chem. A* **2006**, 110, 11359.
- (55) Remko, M.; Van Duijnen, P. T.; von der Lieth, C. W. *THEOCHEM* **2007**, 814, 119.
- (56) Markham, G. D.; Bock, C. L.; Bock, C. W. *Struct. Chem.* **1997**, 8, 293.
- (57) Payaka, A.; Tongraar, A.; Rode, B. M. *J. Phys. Chem. A* **2009**, 113, 3291.
- (58) Leung, K.; Rempe, S. B. *J. Am. Chem. Soc.* **2004**, 126, 344.
- (59) Kameda, Y.; Sasaki, M.; Yaegashi, M.; Tsuji, K.; Oomori, S.; Hino, S.; Usuki, T. *J. Solution Chem.* **2004**, 33, 733.
- (60) da Silva, E. F.; Svendsen, H. F.; Merz, K. M. *J. Phys. Chem. A* **2009**, 113, 6404.
- (61) Gojlo, E.; Smiechowski, M.; Panuszko, A.; Stangret, J. *J. Phys. Chem. B* **2009**, 113, 8128.
- (62) Myshakin, E. M.; Jordan, K. D.; Sibert, E. L.; Johnson, M. A. *J. Chem. Phys.* **2003**, 119, 10138.
- (63) Michaux, C.; Wouters, J.; Perpete, E. A.; Jacquemin, D. *J. Am. Soc. Mass Spectrom.* **2009**, 20, 632.
- (64) Epstein, L. M.; Saitkulova, L. N.; Shubina, E. S. *J. Mol. Struct.* **1992**, 270, 325.
- (65) Wang, X.-B.; Jagoda-Cwiklik, B.; Chi, C.; Xing, X.-P.; Zhou, M.; Jungwirth, P.; Wang, L.-S. *Chem. Phys. Lett.* **2009**, 477, 41.
- (66) Park, J. Y.; Woon, D. E. *Astrophys. J.* **2006**, 648, 1285.
- (67) de Veij, M.; Vandenabeele, P.; De Beer, T.; Remonc, J. P.; Moens, L. *J. Raman Spectrosc.* **2009**, 40, 297.
- (68) Nickolov, Z.; Ivanov, I.; Georgiev, G.; Stoilova, D. *J. Mol. Struct.* **1996**, 377, 13.
- (69) Ito, K.; Bernstein, H. J. *Can. J. Chem.* **1956**, 34, 170.
- (70) Wang, L. Y.; Zhang, Y. H.; Zhao, L. J. *J. Phys. Chem. A* **2005**, 109, 609.
- (71) Kakihana, M.; Kotaka, M.; Okamoto, M. *J. Phys. Chem.* **1983**, 87, 3510.
- (72) Moreno, A. J.; Alegria, A.; Colmenero, J.; Frick, B. *Appl. Phys. A: Mater. Sci. Process.* **2002**, 74, S135.

- (73) Montjoie, A.-S.; Müller-Warmuth, W. *Z. Naturforsch. A* **1985**, *40*, 596.
- (74) Jones, L. H.; McLaren, E. *J. Chem. Phys.* **1954**, *22*, 1796.
- (75) Zachariasen, W. H. *J. Am. Chem. Soc.* **1940**, *62*, 1011.
- (76) Spinner, E. *J. Chem. Soc. B* **1967**, 874.
- (77) Beckmann, L.; Gutjahr, L.; Mecke, R. *Spectrochim. Acta* **1964**, *20*, 1295.
- (78) Ernstbrunner, E. E.; Girling, R. B.; Hester, R. E. *J. Chem. Soc., Faraday Trans.* **1978**, *74*, 1540.
- (79) Halgren, T. A. *J. Comput. Chem.* **1996**, *17*, 490. The MMFF94 parameter files can be accessed at <http://www.mrw.interscience.wiley.com/suppmat/0192-8651/suppmat/aid.0176.html> (accessed 06/10/2009).
- (80) Rowsell, J. L. C.; Yaghi, O. M. *Microporous Mesoporous Mater.* **2004**, *73*, 3.
- (81) Li, H.; Eddaoudi, M.; O'Keeffe, M.; Yaghi, O. M. *Nature* **1999**, *402*, 276.
- (82) Chui, S. S. Y.; Lo, S. M. F.; Charmant, J. P. H.; Orpen, A. G.; Williams, I. D. *Science* **1999**, *283*, 1148.
- (83) Rakitin, A. R.; Pack, G. R. *Langmuir* **2005**, *21*, 837.
- (84) Woo, H.-K.; Wang, X.-B.; Kiran, B.; Wang, L.-S. *J. Phys. Chem. A* **2005**, *109*, 11395.
- (85) Gould, S. L.; Tranchemontagne, D.; Yaghi, O. M.; Garcia-Garibay, M. A. *J. Am. Chem. Soc.* **2008**, *130*, 3246.
- (86) Winston, E. B.; Lowell, P. J.; Vacek, J.; Chocholousova, J.; Michl, J.; Price, J. C. *Phys. Chem. Chem. Phys.* **2008**, *10*, 5188.
- (87) Barreto, L. S.; Mort, K. A.; Jackson, R. A.; Alves, O. L. *J. Phys.: Condens. Matter* **2000**, *12*, 9389.
- (88) Deeth, R. J. *Inorg. Chem.* **2008**, *47*, 6711.

CT900304Q